Single Layer Anisotropic Impedance Surface for Linear to Circular Polarization Conversion in Reflect Mode

[*]Efstratios Doumanis, [*]George Goussetis, [+]Jose-Luis Gómez-Tornero, [*]Robert Cahill, and [*]Vincent Fusco

[*]*Queen's University of Belfast*
University Road Belfast, BT7 1NN, Northern Ireland, UK
edoumanis01@qub.ac.uk, g.goussetis-v.fusco@ecit.qub.ac.uk, r.cahill@ee.qub.ac.uk

[+]*Department of communication and Information Technologies, Technical University of Cartagena*
Cartagena, 30202, Spain
josel.gomez@upct.es

***Abstract*—Anisotropic impedance surfaces are proposed as low-profile and broadband linear to circular polarization reflectors. By virtue of anisotropy it is possible to independently control the reflection characteristics of two orthogonal linearly polarized incident plane waves and therefore achieve polarization conversion. By means of an example involving a dipole array, the operation principle is demonstrated. A prototype is designed and its performance characteristics are evaluated. The 3 dB relative axial ratio bandwidth exceeds 60 %, while low loss and better than previously reported angular stability are also demonstrated. Numerical and experimental results on a fabricated prototype are presented to validate the design and the performance.**

I. Introduction

Polarization converters are key elements in sensor applications and mm-wave systems. They are employed in millimeter-wave and sub-millimeter wave imaging applications [1]. In satellite systems, polarization converters are used to minimize the effect of Faraday rotation caused by the ionosphere [2]. They have been used in the design of circulators [3] and isolators [1], [4] as well as for remote environmental monitoring applications [5]. Polarization transformers are also important in antenna applications where polarization diversity is highly desired [6]. Various polarization converter structures have been presented to date [1], [3]-[11]. A variety of all-metal structures suitable for sub-millimeter wave frequencies polarization conversion were presented in [10]. They are based on double layer aperture frequency selective surfaces (FSS). An all-metal double layer array of split slot rings employed in a quasi-circulator for RCS characterization was reported in [3].

All of the polarization converter surfaces reported above consist of multilayer planar arrays. This increases bulkiness, due to the need for multilayer structures with layers commonly placed quarter wavelength apart, as well as the fabrication complexity and associated costs. A single layer split slot ring LP to circular polarization (CP) converter design was reported in [5], which however reflects approximately 3 dB of the incoming power leading to high insertion loss. Additionally all the above designs operate in the transmit mode.

In [11] the use of polarizers in mm-wave imaging systems is described. In this system [1, 11], schematically shown in Fig. 1, it would be beneficial to combine the reflector and the polarization converter in a single component that could perform both operations. This would significantly reduce system complexity by replacing the linear to circular polarization transformer and the scanning mirror (block P in Fig. 1) by a linear to circular polarizing reflector (block P' in Fig. 1). A linear to circular polarization reflector has been proposed in [12]. This design involves two grids, one for each of the two orthogonal polarizations of the incident wave, placed λ/8 apart. Although simple in concept, this solution is of severely limited usage due to its inherent narrow-band operation and poor angular stability.

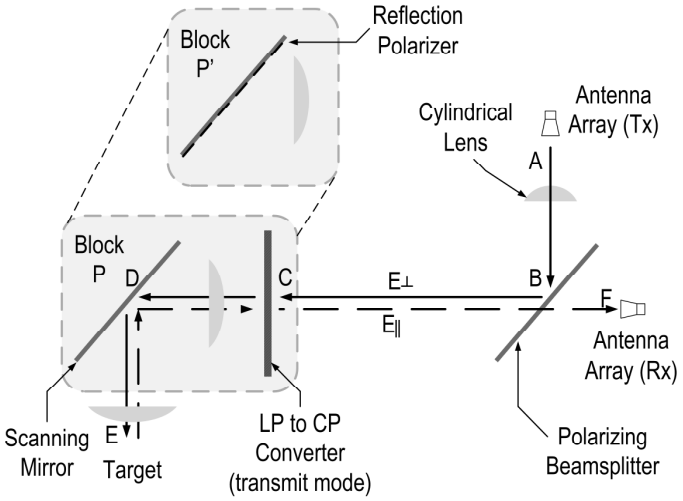

Fig. 1. Simplified block diagram of an imaging mm-wave system. Proposed replacement of the scanning mirror and LP to CP converter by a reflection polarization transformer.

Doubly periodic planar metallo-dielectric arrays have over the past decade been extensively studied in the literature as engineered impedance surfaces [13-19]. When supported by a ground plane, and neglecting thermal losses or grating lobes,

these structures fully reflect incident plane waves in a specular direction with a tailored phase shift. Among those surfaces, anisotropic designs impose a differential phase shift to the two polarizations of the incoming plane wave [20-21].

In this paper we propose a new type of single layer, low-profile anisotropic impedance surface that reflects incoming linearly polarized waves to outgoing circularly polarized waves. Advantages of the proposed reflection polarizer include low-profile, mass and size, wide-band operation, low-loss and angular stability. The proposed structure is also compatible with conventional single layer PCB technology, thus minimizing the associated costs and allowing scalability to mm-waves. Numerical and experimental results are presented to demonstrate the performance characteristics.

II. Principle of Operation

The polarization of a plane wave refers to the orientation of the electric field vector, which may be in a fixed direction or may change with time. Circular polarization is characterized by electric field where the two orthogonal components are of the same amplitude and 90° (or odd multiples of) out of phase [22]. A linearly polarized wave may be converted to a circularly polarized wave by means of an engineered reflector which provides this difference in phase between two crossed linear components. Here we propose to convert linear to circular polarization by means of the differential reflection phase provided by an anisotropic impedance surface. For simplicity here we assume that the impedance surface consists of a double periodic dipole array printed on a grounded dielectric substrate.

Without loss of generality we assume a linearly polarized plane wave from the z>0 half space incident on the surface which lies on the xy-plane. The incidence plane is assumed to be normal to the y-axis (xz-plane) and the direction of propagation (wavenumber) of the incoming wave is at an angle θ with the z-axis (Fig. 2). Two orthogonal linearly polarized plane waves suitable for the expansion of the incoming and outgoing waves are defined by electric and magnetic fields transverse to the xz-plane respectively. For θ≠0, these are commonly referred to as TE and TM polarizations and are schematically depicted in Fig. 2. Next assume that the incoming wave is polarized at $\xi = 45^{\circ}$ with respect to the y-axis. Such a wave consists of a superposition of a TE and a TM wave with equal magnitude and phase.

If the surface is lossless and no grating lobes exist, both the TE and TM components will be fully reflected in the specular direction. The condition for the outgoing wave to have circular polarization is therefore that the impedance surface imposes a differential reflection phase of 90° (or odd multiples of) to the TE and TM component. In particular, the reflected wave will be characterized by left-handed circular polarization (LHCP) if the TE component is reflected with 90° (±360°) phase advance with respect to the TM component, and right-handed circular polarization (RHCP) if the TM component is reflected with 90° (±360°) phase advance with respect to the TE component. Similar conditions hold for the reflection phases of the x- and y-polarized components for normally incident plane waves (θ=0), where TE and TM polarizations are not formally defined.

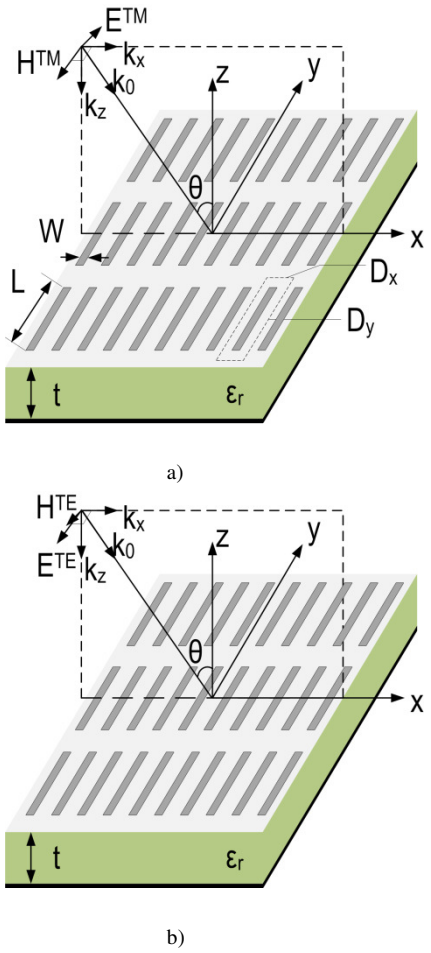

Fig. 2. TM (a) and TE (b) incidence on an anisotropic impedance surface consisting of a dipole-FSS printed on a grounded dielectric slab. Geometrical configuration.

In order to demonstrate the operation principle of the proposed design we employ an example. In the following a dielectric substrate with permittivity εr=3.5 and thickness of t=1.524 mm is considered for a linear to circular polarization converter within the 10-15 GHz band. The angle of incidence is θ=45° as exemplified in the schematic of Fig. 1. CST Microwave Studio was employed for the full-wave simulations. Metallic and dielectric losses are accounted for in the simulations. In particular, the loss tangent of the substrate is tanδ= 0.0018 and the conductivity of copper is used for the metal dipoles. The thickness of the dipoles and of the ground plane is assumed to be 35 μm. The dimensions of the design are given in the legend of Fig. 3. Referring to Fig. 3, the dimensions are L= 7.0 mm, W= 0.5mm, Dy=8.0 mm and Dx=1.0 mm. An axial ratio requirement of less than 1.5 dB as well as fabrication tolerance constraints have been considered during the optimization.

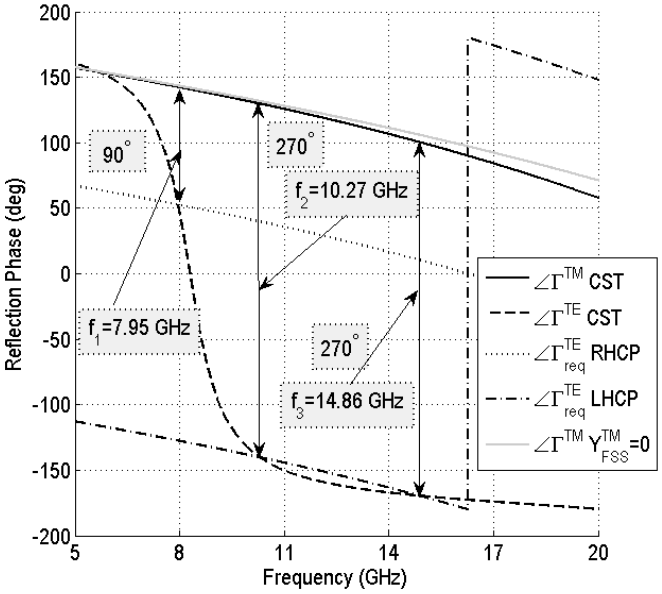

Fig. 3. Full wave reflection phase for plane waves incident at θ=45° onto a dipole array with dimensions (in mm): L=7.0, W=0.5, D_y=8.0 and D_x=1.0 printed on a substrate with thickness t=1.524 mm and relative permittivity ε_r=3.5 for TM (solid line) and TE (dashed line) polarizations. Required reflection phase of the TE component for RHCP (dotted line) and LHCP (dash-dotted line). Reflection phase of the TM polarized incident wave for the case of an un-patterned grounded dielectric (grey solid line).

The reflection phase $\angle\Gamma^{TM}$ of the TM polarized incident wave for the case of an un-patterned grounded dielectric has been obtained analytically and is plotted in Fig. 3 (grey solid line). The reflection phase in the presence of the array as obtained using full-wave simulation is superimposed in Fig. 3 for comparison (solid line). The discrepancy between the two curves is attributed to the approximation of an open circuit for the dipole array upon TM illumination. As it can be seen in Fig. 3, the open circuit approximation is increasingly accurate for lower frequencies.

The required reflection phase, $\angle\Gamma_{req}^{TE}$, that will convert incident linear polarization to RHCP and LHCP can be obtained by subtracting 90° and 270° respectively from the full-wave reflection Γ^{TM}. The relevant curves are plotted in Fig. 3 (dotted line and dash-dotted lines respectively). In view of Fig. 3, at frequency f_1=7.95 GHz, the difference between the reflection phase experienced by the TE and TM components is 90° which results in a right-hand circularly polarized wave (RHCP). At frequencies f_2=10.27 GHz and f_3=14.82 GHz the phase difference is 270° and the reflected wave is left-hand circularly polarized (LHCP). Due to the smooth variation of the reflection phases for both polarizations between these two frequencies, a small variation of the axial ratio is anticipated within this range.

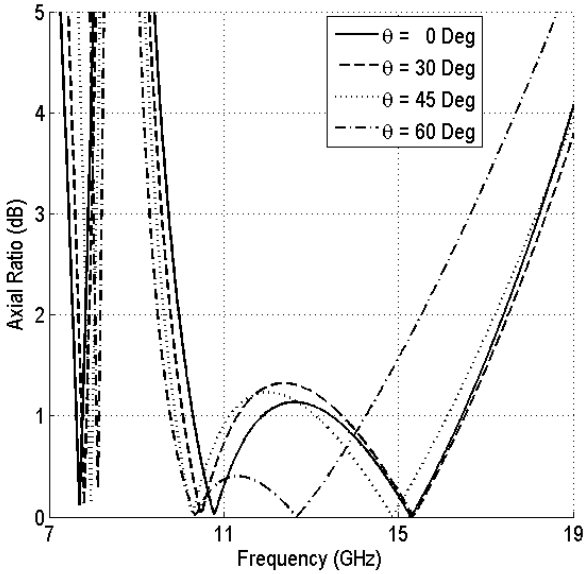

Fig. 4. Simulated axial ratio (dB) of the reflected wave from the array of Fig. 3 for incident plane wave linearly polarized at ξ= 45° at incidence angles θ=0° (solid line), θ=30° (dashed line), θ=45° (dotted line), and θ=60° (dash-dotted line).

The simulated reflection loss is small and comparable for the two polarizations. The maximum reflection loss is 0.2 dB and is observed for the TE polarization at 8.29GHz, where reflection phase is 0°. This frequency, associated with Artificial Magnetic Conductor operation, is known to exhibit stronger resonance phenomena [14] and therefore thermal losses peak around that frequency. Significantly, the frequency range of interest lies outside strong resonance phenomena and therefore the losses for both polarizations are small. For frequencies between 10.5 to 20 GHz, the thermal loss for both components results to less than 0.04 dB reduction in the reflection coefficient. The grating lobe region is well above the operational frequency range of the polarization converter for all angles of incidence considered. The above suggest that the assumption of full specular reflection for both polarizations is valid to a good extend and therefore to a good approximation the design can be based on the reflection phases. We note that in case this assumption does not hold, a higher absorption of either polarization can be compensated by tilting the incoming wave polarization angle with the y-axis, ξ, to values different than 45°, thus increasing the relative strength of the component that experiences higher losses.

The axial ratio as obtained from the full-wave simulations for this array for incidence angle θ= 45°, is shown in Fig. 4 (dotted line). The 3 dB axial ratio bandwidth is more than 63%, while the 1.5 dB axial ratio bandwidth is over 52%. The minimum axial ratio for RHCP is 0.16 dB at 7.95 GHz. For LHCP, two minimum points are observed at 10.27 GHz and 14.86 GHz where the simulated axial ratio is 0.03 dB and 0.006 dB respectively. These frequencies exactly coincide with the frequencies f_1, f_2 and f_3 of Fig. 3. Fig. 4 also shows the axial ratio for various angles of incidence between 0° and

60°. The 3 dB axial ratio bandwidth for θ=0° (solid line), 30° (dashed line), and 60° (dash-dotted line) are 60.8 %, 63.1 %, and 56.6 %, respectively. Within the 9.85 GHz to 16.5 GHz band the axial ratio is below 1.5 dB for all angles of incidence with exception grazing incidence at 60°. The low profile of the structure together with the reported levels of polarization purity over a large bandwidth and angular field-of-view is a significant improvement compared to the state of the art [1].

III. Experimental Validation

In order to experimentally validate the above, a prototype array has been fabricated and measured. The array has been photo-etched on a Taconic RF-35 laminate with a relative dielectric permittivity ε_r=3.5, loss tangent tanδ=0.0018 and thickness t=1.524 mm. The thickness of the copper dipole elements and ground plane is 35 μm. The prototype array consists of 272x34 elements with overall dimensions 30x30 cm. A photograph of the prototype is shown in Fig. 5 (a).

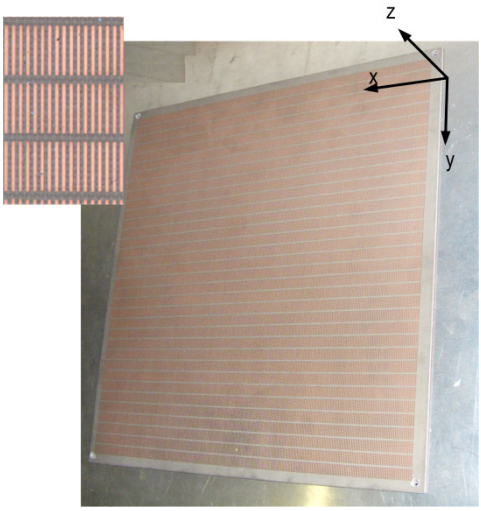

(a)

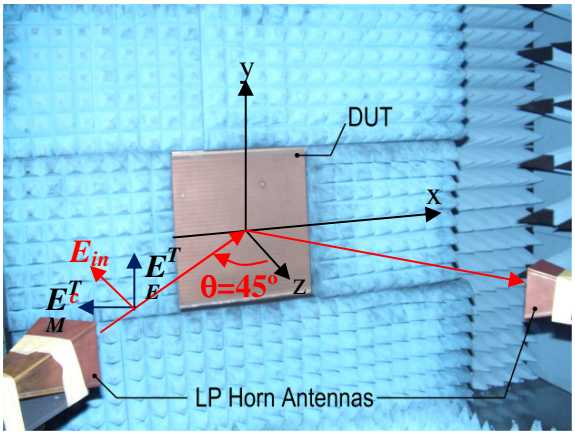

(b)

Fig. 5. (a) Photograph of the fabricated prototype (part of the array zoomed as an inset) and (b) the measurement setup.

Standard-gain X-band horn antennas are used as the receiver and transmitter. A linearly polarized horn antenna (Tx) is fed from a Vector Network Analyzer (VNA) and positioned at θ= 45° angle to the screen at normal incidence. The array is positioned at a distance of 60 cm away from the two antennas. The reflection phase in the far field is taken using the horn antennas and is then normalized with respect to an identical measurement where the array is substituted by a fully metallic surface. TE and TM incidence is achieved by relative rotation of the horn antennas by 90°. A photograph of the measurement setup is shown in Fig. 5 (b) for TE incidence. The measured axial ratio up to 13 GHz is plotted in Fig. 6 along with the simulated one as obtained with CST for comparison. The measured response is in good agreement with the simulation. Some discrepancies are attributed to experimental tolerances.

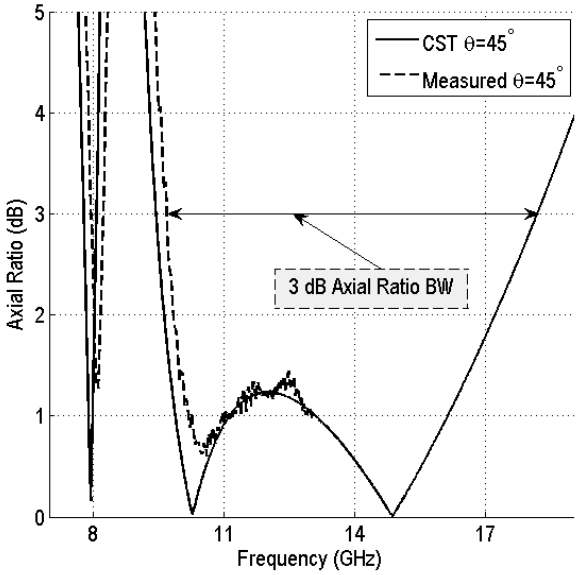

Fig. 6. Measured axial ratio of the fabricated design for plane wave angle of incidence θ=45° (dotted line). The simulation for θ=45° is repeated from Fig. 5for comparison.

IV. Conclusion

A single-layer anisotropic impedance surface for linear to circular polarization conversion upon reflection has been presented. The basic principle of operation has been demonstrated, and by means of an example design the performance is assessed. The 3 dB axial ratio for the given example was in excess of 60% over a wide angular bandwidth. Full-wave numerical and experimental results have been presented that demonstrate the LP to CP conversion performance of the proposed design.

Acknowledgment

The authors would like to thank Dr. Duncan Robertson for fruitful discussions and Taconic Advanced Dielectric Division for providing the substrate. The authors wish to acknowledge Mr Gerry Rafferty for fabricating the prototype.

REFERENCES

[1] Dietlein, A. Luukanen, Z. B. Popovic, and E. Grossman, "A W-Band polarization converter and isolator," IEEE Trans. Antennas Propag., vol. 55, no. 6, pp. 1804-1809, Jun. 2007.

[2] G. Maral, M. Bousquet, Satellite communications systems, Systems, techniques and technology. Sussex, Wiley, 2009, ch. 5, pp. 208.

[3] M. Euler and V. Fusco, "Split slot ring spatial quasi-circulator for RCS characterization," Electronic Lett., vol. 46, no. 6, pp. 394-395, Mar. 2010.

[4] S. Hollung, W. A. Shiroma, M. Markovic, and Z. B. Popovic, "A quasi-optical isolator," IEEE Microw. Guided Wave Lett., vol. 6, no. 5, pp. 205-206, May 1996.

[5] M. Euler, V. Fusco, R. Cahill, and R. Dickie, "325 GHz single layer sub-millimeter wave FSS based split ring linear to circular polarization convertor," IEEE Trans. Antennas Propag., vol. 58, no. 7, pp. 2457-2459, Jul. 2010.

[6] K. S. Min, J. Hirokawa, K. Sakurai, M. Ando, and N. Goto, "Single-layer dipole array for linear-to-circular polarization conversion of slotted waveguide array," IEE Proc. Microw. Antennas Propag., vol. 143, no. 3, Jun. 1996.

[7] D. S. Lerner, "A wave polarization converter for circular polarization," IEEE Trans. Antennas Propag., vol. 13, no. 1, pp. 3-7, Jan. 1965.

[8] L. Young, L. A. Robinson, and C. A. Hacking, "Meander-line Polarizer," IEEE Trans. Antennas Propag., vol. 21, no. 3, pp. 376-378, May 1973.

[9] T. K. Wu, "Meander-line polarizer for arbitrary rotation of linear polarization," IEEE Microw. Guided Wave Lett.. vol. 4, no. 6, pp. 199-201, Jun. 1994.

[10] M. Euler, V. Fusco, R. Cahill, R. Dickie, "Sub-millimetre wave linear to circular polarization converter study," in Proc. Eur. Microw. Conf., Rome, Italy, Sep. 2009, pp. 2892–2895.

[11] K. M. K. H. Leong, W. A. Shiroma, "Waffle-grid polarizer," Electronic Lett., vol. 38, no. 22, pp. 1360-1361, Oct. 2002.

[12] H. Meikle, Modern Radar Systems. Norwood, Artech House, 2008, ch. 5, pp. 147-152.

[13] D. Sievenpiper, Z. Lijun, R. F. Broas, N. G. Alexopoulos, and E. Yablonovitch, "High-impedance electromagnetic surfaces with a forbidden frequency band," IEEE Trans Microw. Theory Tech., vol. 47, no. 11, pp. 2059–2074, Nov. 1999.

[14] G. Goussetis, A.P. Feresidis, J.C. Vardaxoglou, "Tailoring the AMC and EBG Characteristics of Periodic Metallic Arrays Printed on Grounded on Grounded Dielectric Substrate," IEEE Trans. Antennas Propag., vol. 54, no. 1, pp. 82-89, Jan. 2006.

[15] O. Luukkonen, C. R. Simovski, G. Granet, G. Goussetis, D. Lioubtchenko, A. Raisanen, S. A. Tretyakov, "Simple and accurate analytical model of planar grids and high-impedance surfaces comprising of metal strips or patches," IEEE Trans. Antennas Propag., vol. 56, no. 6, pp. 1624-1632, Jun. 2008.

[16] G. Goussetis, J. L. Gomez-Tornero, A. P. Feresidis, and N. Uzunoglu "Artificial Impedance Surfaces for reduced dispersion in Antenna Feeding Systems," IEEE Trans. Antennas Propag., vol. 54, no. 1, pp. 82-89, Jan. 2006.

[17] A. Feresidis, G. Goussetis, S. Wang, and J. C. Vardaxoglou, "Artificial Magnetic Conductor Surfaces and their application to low profile high-gain planar antennas," IEEE Trans. Antennas Propag., vol. 53, no. 1, pp. 209-215, Jan. 2005.

[18] S. Wang, A. P. Feresidis, G. Goussetis, and J. C. Vardaxoglou, "High-gain subwavelength resonant cavity antennas based on metamaterial ground planes," IEE Proc. Microw. Antennas Propag., vol. 153, no. 1, pp. 1-6, Feb. 2006.

[19] G. Goussetis, A.P. Feresidis, A. Yakovlev and C. Simovski, "High Impedance Surfaces," chapter 31 in Metamaterial Handbook vol. I, Taylor and Francis, ISBN: 97-814-2005-3623

[20] S. Maci, M. Caiazzo, A. Cucini, and M. Casaletti, "A Pole-Zero Matching Method for EBG Surfaces Composed of a Dipole FSS Printed on a Grounded Dielectric Slab," IEEE Trans. Antennas Propag., vol. 53, no. 1, pp. 70-81, Jan. 2005.

[21] G. Goussetis, and A. P. Feresidis, "Perturbed frequency selective surfaces for multiband high impedance surfaces," IET Microw. Antennas Propag., vol. 4, no. 8, pp. 1105-1110, 2010.

[22] B. Toh, R. Cahill, and V. Fusco "Understanding and measuring circular polarization," IEEE Trans. Education, vol. 46, no. 3, pp. 313-318, Aug. 2003.